Drug Design, Development and Therapy

Dovepress
open access to scientific and medical research

Open Access Full Text Article

ORIGINAL RESEARCH

Prostate Cancer Therapy Using Docetaxel and Formononetin Combination: Hyaluronic Acid and Epidermal Growth Factor Receptor Targeted Peptide Dual Ligands Modified Binary Nanoparticles to Facilitate the in vivo Anti-Tumor Activity

Zhaoqiang Dong[1], Yuzhen Wang[2], Jing Guo[3], Chuan Tian[4], Wengu Pan[4], Hongwei Wang[4], Jieke Yan[4]

[1]Department of Cardiology, The Second Hospital of Shandong University, Ji'nan, 250033, People's Republic of China; [2]Clinical Department, Jinan Vocation College of Nursing, Ji'nan, 250033, People's Republic of China; [3]Department of Gynaecology, The Second Hospital of Shandong University, Ji'nan, 250033, People's Republic of China; [4]Department of Renal Transplantation, The Second Hospital of Shandong University, Ji'nan, 250033, People's Republic of China

Correspondence: Jieke Yan, Department of Renal transplantation, The Second Hospital of Shandong University, No. 247 Beiyuan Street, Ji'nan, 250355, People's Republic of China, Email yanjiekesdu@163.com

Objective: To evaluate the prostate cancer therapy efficiency of the synergistic combination docetaxel (DTX) and formononetin (FMN) in one nano-sized drug delivery system. Hyaluronic acid (HA) and epidermal growth factor receptor-targeted peptide (GE11) dual ligands were applied to modify the nano-systems.

Methods: In this study, GE11-modified nanoparticles (GE-NPs) were applied for the loading of DTX, and HA-decorated NPs (HA-NPs) were used to encapsulate FMN. HA and GE11 dual ligand-modified binary nanoparticles (HAGE-DTX/FMN-NPs) were constructed by the self-assembling of GE-NPs and HA-NPs. The anti-PCa ability of the system was evaluated in vitro on PC-3 human prostate carcinoma cells (PC3 cells) and in vivo on PC3 tumor-bearing mice in comparison with single NPs and free drugs formulations.

Results: HA/GE-DTX/FMN-NPs were nano-sized particles with smaller particles coating on the inner core and achieved a size of 189.5 nm. HA/GE-DTX/FMN-NPs showed a cellular uptake efficiency of 59.6%, and a more efficient inhibition effect on PC3 cells compared with single ligand-modified NPs and free drugs. HA/GE-DTX/FMN-NPs showed significantly higher tumor inhibition efficiency than their single drug-loaded counterparts and free drugs.

Conclusion: HA/GE-DTX/FMN-NPs have a synergistic anti-tumor effect and also could the reduce unexpected side effects during the cancer therapy. It could be used as a promising anti-PCa system.

Keywords: prostate cancer, docetaxel, formononetin, hyaluronic acid, epidermal growth factor receptor, binary nanoparticles

Introduction

Prostate cancer (PCa) is the second most commonly diagnosed cancer (20% of male new cancer cases) and the fifth leading cause of cancer death in males (9.8% of male cancer deaths).[1,2] Androgen-deprivation therapy (ADT) is the initial treatment of metastatic PCa involving surgical castration or medical castration.[3,4] However, metastatic PCa will inevitably progress to metastatic castration-resistant prostate cancer (mCRPC).[5] Based on several phase III clinical trials, every-3-week docetaxel with concurrent steroid is the preferred first-line chemotherapy treatment for men with symptomatic mCRPC.[4,6,7]

Docetaxel (DTX), an approved antineoplastic agent, can enhance tubulin polymerization and inhibit microtubule depolymerization, which results in the inhibition of mitosis in cells and achieves anti-tumor effect. However, due to its

Received: 16 March 2022
Accepted: 27 July 2022
Published: 11 August 2022

drug resistance and insolubility (4.93 μg/mL in water), combination therapy and diverse anti-cancer nano-drug delivery systems were engineered for inhibition of aforementioned drawbacks.[8–10] The synergy of action mechanism is the prerequisite of combination therapy, and the combination of DTX and Chinese traditional medicine has become the focus of research, such as DTX and Fuzheng Yiliu decoction whose principal component is formononetin (FMN).[11–14]

FMN, a methoxylated isoflavone [7-hydroxy-3-(4-methoxypheny)-4H-1-benzopyran-4-one], can be mainly extracted from red clover (*Trifolium pratense*) and the Chinese medicinal plant *Astragalus membranaceus*.[15] FMN is insoluble in water and has been used as one of the fundamental herbs for the treatment of cancer in China.[14] The therapeutic prospect of FMN in treating prostate cancer, especially for castration-resistant prostate cancer, has been evidenced in several cell culture systems and human xenograft mouse models.[14,16] The mechanism of FMN, which induced cytotoxicity in prostate cancer cells, contains two factions, apoptosis and G1 cell cycle arrest.[17] Specifically, apoptosis is due to upregulation of dexamethasone-induced retrovirus-associated DNA sequences (Ras)-related protein 1 (RASD1), Bcl-2-associated protein (Bax), caspase-3, and PARP (poly-ADP ribose polymerase); reduction of B-cell lymphoma 2 (Bcl-2) levels; inhibition of insulin-like growth factor 1 (IGF-1) receptor androgen-independent pathway; increased phosphorylation of p38, and blocked AKT (protein kinase B) phosphorylation accompanied by growth in Bax/Bcl-2 ratio.[18–20] G1 cell cycle arrest is due to suppression of the oncogenic PI3K/AKT pathway, downregulation of cyclin D1, AKT, and cyclin-dependent kinase 4 (CDK4).[21]

Recent researches have indicated that epidermal growth factor receptor (EGFR) was detectable in most patients with prostate cancer.[22] Our previous study has developed EGFR peptide (GE11)-targeted, pH-sensitive nanoparticles (GE NPs) for PCa therapy.[23] Hyaluronic acid (HA) was reported to modify nanoparticles (NPs) to facilitate the delivery to prostate tumor xenografts.[24] An HA-decorated, cabazitaxel and orlistat co-loaded nano-system was developed by researchers to treat prostate cancer.[25]

In this study, GE-NPs were applied for the loading of DTX, and HA-decorated NPs (HA-NPs) were used to encapsulate FMN. HA and GE11 dual ligand-modified binary nanoparticles were constructed by the self-assembling of GE-NPs and HA-NPs. The anti-PCa ability of the system was evaluated in vitro and in vivo in comparison with single NPs and free drug formulations.

Materials and Methods

Materials and Animals

DTX, FMN, dimethyldioctadecylammonium bromide (DDAB), coumarin-6, carbopol 940 (CP), and (3-[4,5-dimethyl-2-thiazolyl]-2,5-diphenyl-2H-tetrazolium) bromide (MTT) were purchased from Sigma-Aldrich Co., Ltd (St Louis, MO). Hyaluronic acid-polyethylene glycol-distearoyl phosphoethanolamine (HA-PEG-DSPE) was provided by Xi'an Ruixi Biological Technology Co., Ltd (Xi'an, China). Poly (lactic-co-glycolic acid) (PLGA, molar ratio of D, L-lactic to glycolic acid, 50:50) was purchased from Ji'nan Daigang Biotechnology Co. Ltd (Ji'nan, China).

Human PC3 prostate adenocarcinoma cell line (PC3 cells) and normal human prostate cell line (RWPE-1 cells) were purchased from American Type Culture Collection (Manassas, VA). Balb/c nude mice (6–8 weeks) were purchased from Shanghai Slack Laboratory Animal Co., Ltd (Shanghai, China). The animal experiments were approved by the Animal Ethics Committee of Shandong University according to the requirements of the National Act on the Use of Experimental Animals (P. R. China).

Preparation of DTX Loaded GE-NPs

DTX-loaded GE-NPs (GE-DTX-NPs, Figure 1A) were prepared using a solvent displacement method using the perilously prepared PLGA-PEG-GE11.[23] Briefly, PLGA-PEG-GE11 (200 mg) and DTX (50 mg) were dissolved in 5 mL acetonitrile/DMSO (50/50, v/v) to form the organic phase, and then added dropwise into 15 mL Milli-Q water containing CP (0.05% w/v) under gentle stirring (400 rpm). Then the product was dialyzed (molecular weight cut-off 3000 Da) against Milli-Q water for one day and filtered through a 0.45 μm membrane to obtain GE-DTX-NPs. Blank GE-NPs were prepared without adding DTX. DTX and FMN co-loaded GE-NPs (GE-DTX/FMN-NPs) were prepared by adding additional FMN (30 mg) to the organic phase.

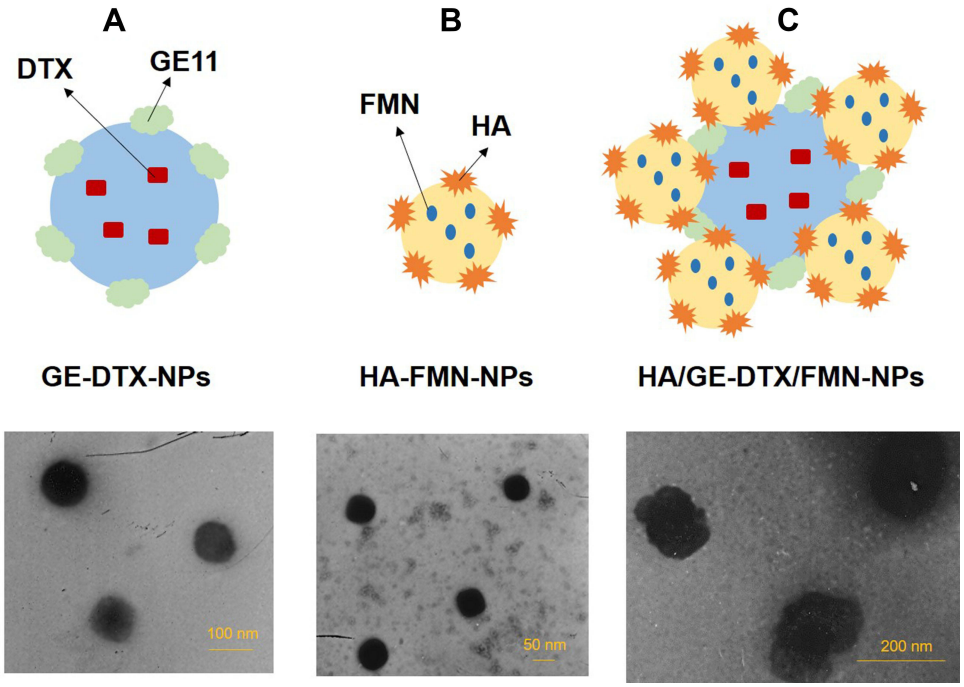

Figure 1 Scheme graphs and TEM images of GE-DTX-NPs (**A**), HA-FMN-NPs (**B**), and HA/GE-DTX/FMN-NPs (**C**).

Preparation of FMN-Loaded HA-NPs

FMN-loaded HA-NPs (HA-FMN-NPs, Figure 1B) were prepared using a solvent evaporation method.[26] HA-PEG-DSPE (100 mg), soya lecithin (50 mg), and FMN (30 mg) were dissolved in chloroform (5 mL) to produce the organic phase, and then added dropwise into 15 mL Milli-Q water containing DDAB (1% w/v) under gentle stirring (400 rpm). Then the mixture was stirred for 10 h to evaporate the organic solvent to obtain HA-FMN-NPs. Blank HA-NPs were prepared without adding FMN. DTX and FMN co-loaded HA-NPs (HA-DTX/FMN-NPs) were prepared by adding additional DTX (50 mg) to the organic phase.

Preparation of HA and GE11 Co-Modified Binary Nanoparticles

HA and GE11 co-modified, DTX and FMN co-loaded binary nanoparticles (HA/GE-DTX/FMN-NPs, Figure 1C) were prepared by adding HA-FMN-NPs suspension dropwise into GE-DTX-NPs suspension under gentle stirring (400 rpm) for 1 h. Blank HA and GE11 co-modified nanoparticles (HA/GE-NPs) were prepared using HA-NPs and GE-NPs instead. The prepared NPs were all stored at 4°C until use.

Characterization of Nanoparticles

The prepared NPs were characterized in terms of morphology, size, surface charge, drug encapsulation efficiency (EE), and drug loading capacity (LC).[27] The morphology of NPs was recorded by transmission electron microscopy (TEM, JEM-1200EX, JEOL, Japan). The size and zeta potential of NPs were recorded by dynamic light scattering using a Malvern ZS90 instrument (Malvern Instruments, Malvern, UK).

The EE and LC of NPs were determined by HPLC (LC-20A, Shimadzu, Japan). Chromatographic separations were carried out using the Unitary C18 column (250 mm × 4.6 mm). DTX concentration was measured at 230 nm with a mobile phase consisting of acetonitrile/water (55:45, v/v) at a flow rate of 1.0 mL/min.[28] FMN concentration was measured at 254 nm with a mobile phase consisting of acetonitrile:methanol (50:50, v/v) and 0.1% acetic acid in the ratio of 90:10 (v/v) at a flow rate of 0.7 mL/min.[15]

Stability of Nanoparticles

Stability of NPs during storage at 4°C and in the presence of serum was evaluated by measuring the changes of size.[29] Storage stability: during storage at 4°C NPs samples were taken out at determined time points and tested. Serum stability: NPs were incubated with phosphate buffers (PBS) containing fetal bovine serum (FBS, 10%, v/v) at 37°C for 72 h. The samples were tested at scheduled times using the methods in the above section.

In vitro Drug Release

The in vitro release study of NPs was performed using the dialysis method.[30] NPs samples were sealed in dialysis bags and immersed in the release medium (0.5% of Tween 80 in PBS, pH 7.4) stirring at a rate of 100 rpm, separately. At determined time points, samples (0.5 mL) were taken from the release media and the drug release were analyzed by the HPLC method described above. After sampling, the dialysis bag was taken out and re-placed into a new container filling with fresh medium.

Cellular Uptake

Coumarin-6 loaded NPs were prepared by adding coumarin-6 (1 mg/mL) into the organic phase.[31] C6-containing GE-DTX/FMN-NPs, HA-DTX/FMN-NPs, HA/GE-DTX/FMN-NPs, and HA/GE-NPs were added to PC3 cells which were previously incubated in a 24-well plate (1×10^5 cells/well) for 24 h. After 2 h, the medium was discarded and the cells were washed three times with D-Hank's solution, then photographed by fluorescence microscopy. The medium containing the formulation was discarded, and the cells were washed with 1 mL of PBS and were detached with trypsin/ethylene diamine tetraacetic acid and analyzed by a flow cytometer (BD Biosciences, San Jose, CA). Signals were amplified in logarithmic mode for fluorescence to determine the positive events by a standard gating technique, the percentage of which was calculated as the events within the gate divided by the total number of events, excluding cell debris.[32]

In vitro Cytotoxicity and Synergistic Effect

In vitro cytotoxicity of NPs was evaluated on PC3 cells and RWPE-1 cells by MTT assay.[33] Briefly, GE-DTX-NPs, GE-NPs, GE-DTX/FMN-NPs, HA-FMN-NPs, HA-NPs, HA-DTX/FMN-NPs, HA/GE-DTX/FMN-NPs, HA/GE-NPs, and free DTX/FMN at different concentrations were added to PC3 cells or RWPE-1 cells which were previously incubated in 96-well plates (3×10^4 cells/well) for 24 h. Then the medium was removed and MTT solution (20 μL, 5 mg/mL in PBS) was added to each well and incubated for another 4 h. DMSO (200 μL) was added, and the absorbance at 570 nm was recorded. The synergistic effect of HA/GE-DTX/FMN-NPs over GE-DTX-NPs and HA-FMN-NPs was evaluated by Chou–Talalay method,[34] in which the combination index (CI) is introduced for the evaluation of synergistic effect of drugs calculated by the equation: $CI = \sum_{i=1}^{n} (C)i/(Cx)$i. $(C)_i$: the concentrations of drugs in the combination; $(Cx)_i$: the concentrations of drugs used alone. CI less than 1 indicates synergy, closer to zero means stronger synergy efficiency.

In vivo Anti-Tumor Efficacy and Biodistribution

PCa-bearing xenografts were prepared by injecting PC3 cells (5×10^6 cells/100 μL) subcutaneously into the right flank of the Balb/c nude mice, waiting for the tumor to reach about 100 mm^3.[35] Mice were then randomly divided into 8 groups (8 mice per group), treated with GE-DTX-NPs (DTX 10 mg/kg), GE-DTX/FMN-NPs (DTX 5 mg/kg, FMN 3 mg/kg), HA-FMN-NPs (FMN 6 mg/kg), HA-DTX/FMN-NPs (DTX 5 mg/kg, FMN 3 mg/kg), HA/GE-DTX/FMN-NPs (DTX 5 mg/kg, FMN 3 mg/kg), HA/GE-NPs, free DTX/FMN (DTX 5 mg/kg, FMN 3 mg/kg), and 0.9% saline every 3 days by tail injection. Tumor volumes were measured and calculated every 3 days using the formula: (The longest diameters × the shortest diameters^2)/2. Tumors were isolated and photographed at the end of study.

PCa-bearing xenografts were randomly divided into 4 groups (8 mice per group) and injected with GE-DTX/FMN-NPs (DTX 5 mg/kg, FMN 3 mg/kg), HA-DTX/FMN-NPs (DTX 5 mg/kg, FMN 3 mg/kg), HA/GE-DTX/FMN-NPs (DTX 5 mg/kg, FMN 3 mg/kg), and free DTX/FMN (DTX 5 mg/kg, FMN 3 mg/kg) through the tail vein. After 24 h, mice blood and tissues were collected and digested with concentrated nitric acid.[28] Then the tissue samples were diluted with distilled water and analyzed using the method described in the "Drug entrapment and release study" part.

Table 1 Characterization of Nanoparticles

NPs	Size (nm)	PDI	Zeta Potential (mV)	DTX EE (%)	FMN EE (%)	DTX LC (%)	FMN LC (%)
GE-DTX-NPs	100.3±2.9	0.21±0.03	−21.7±1.6	82.7±2.8	N/A	10.3±0.9	N/A
GE-NPs	102.1±2.3	0.15±0.04	−22.3±1.8	N/A	N/A	N/A	N/A
GE-DTX/FMN-NPs	98.9±3.1	0.18±0.03	−19.5±2.1	81.9±2.3	84.1±2.5	9.3±1.2	6.7±1.0
HA-FMN-NPs	43.1±1.7	0.11±0.02	+33.9±2.1	N/A	83.1±2.7	N/A	7.3±0.8
HA-NPs	40.5±1.3	0.10±0.02	+28.6±2.5	N/A	N/A	N/A	N/A
HA-DTX/FMN-NPs	41.4±1.5	0.14±0.03	+31.3±2.4	80.5±2.7	84.3±2.9	9.6±1.1	6.3±1.1
HA/GE-DTX/FMN-NPs	189.5±3.3	0.18±0.05	+19.7±2.3	82.3±2.4	81.9±2.3	8.9±1.5	5.9±1.3
HA/GE-NPs	187.9±3.5	0.21±0.04	+21.1±2.6	N/A	N/A	N/A	N/A

Statistical Analysis

Results were expressed as a mean ± standard deviation (SD). Statistical analysis was performed using an unpaired *t* test (between two groups) or one way analysis of variance (ANOVA) (among three or more groups), and $P < 0.05$ was considered statistically significant.

Results

Characterization of Nanoparticles

The morphology of GE-DTX-NPs, HA-FMN-NPs, and HA/GE-DTX/FMN-NPs is presented in Figure 1. GE-DTX-NPs and HA-FMN-NPs showed spherical appearance, while HA/GE-DTX/FMN-NPs exhibited some smaller particles coating on the inner core. Particle size, zeta potential, EE, and LC of NPs are summarized in Table 1. The size of GE-DTX/FMN-NPs, HA-DTX/FMN-NPs, and HA/GE-DTX/FMN-NPs was 98.9 ± 3.1, 41.4 ± 1.5, and 189.5 ± 3.3 nm, respectively. Surface of GE-NPs was negative: −22.3±1.8 mV. When incubating with positively charged HA-NPs (+28.6±2.5), the resulting HA/GE-NPs showed positive zeta potential (+21.1±2.6). The EEs of NPs were over 80%. The size of NPs remained stable during 3 months of study and 72 h in the presence of serum (Figure 2), illustrating the good stability of the systems.

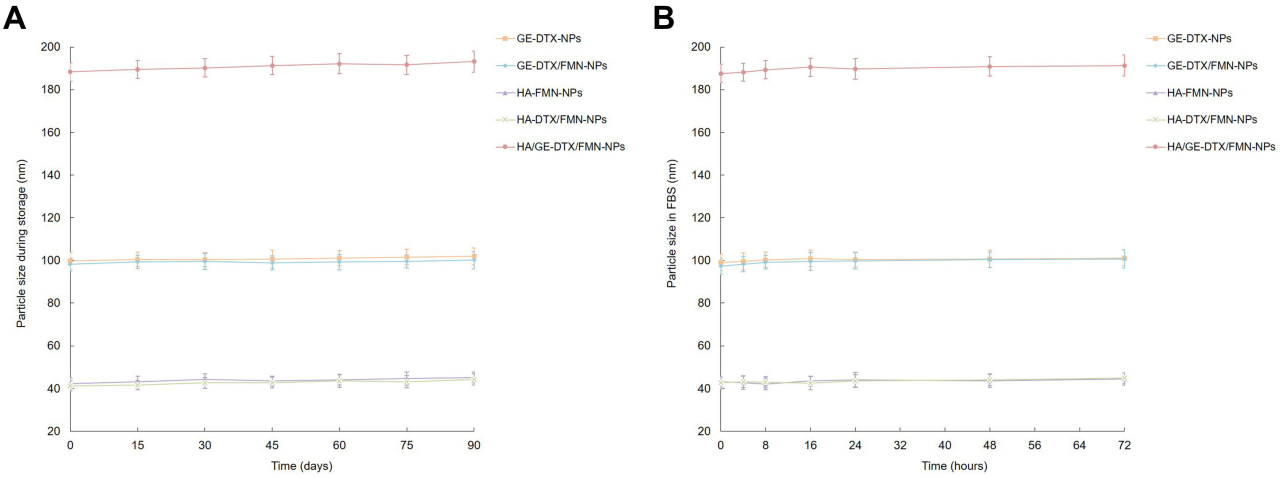

Figure 2 Stability of NPs during storage at 4°C (**A**), and in the presence of fetal bovine serum (FBS, 10%, v/v) at 37°C for 72 h (**B**). Data are presented as means ± standard deviation (*n*=3).

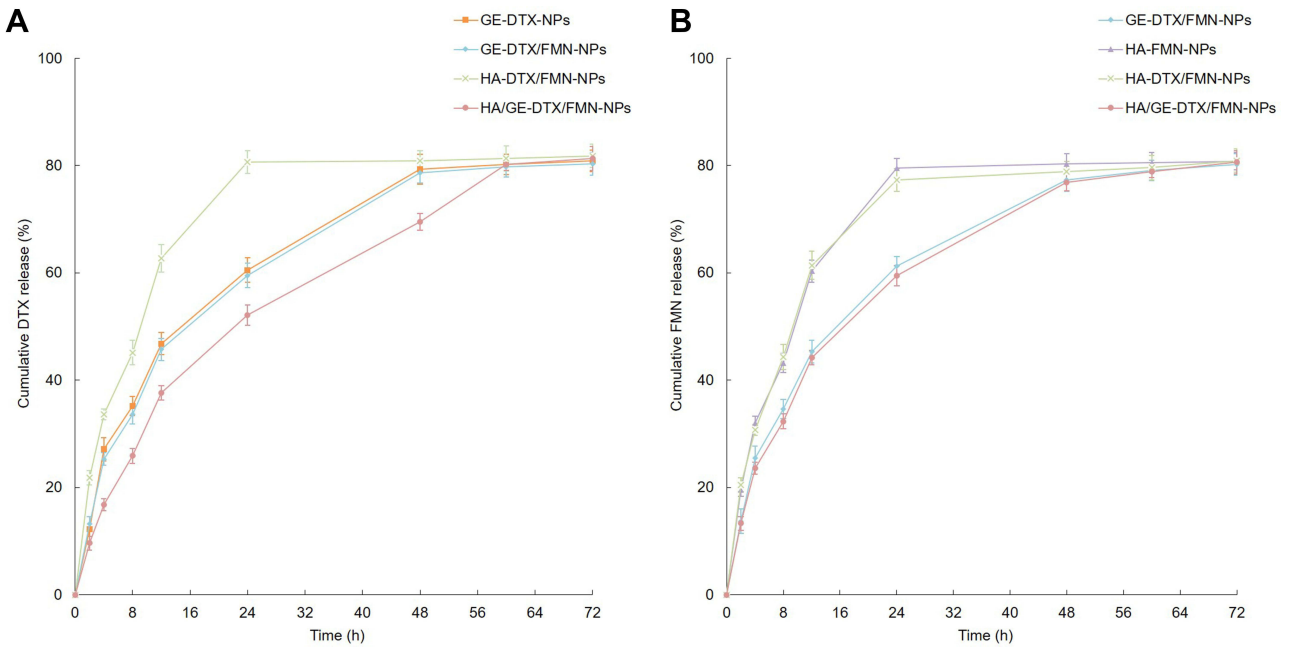

Figure 3 In vitro DTX (**A**) and FMN (**B**) release performed using dialysis method. Data are presented as means ± standard deviation (*n*=3).

In vitro Drug Release

The in vitro drug release rate from different NPs was in sustained behavior but not in the same pattern (Figure 3). DTX release from HA/GE-DTX/FMN-NPs was slower than from GE-DTX/FMN-NPs, and the latter was slower than that of HA-DTX/FMN-NPs. However, FMN release from HA/GE-DTX/FMN-NPs and GE-DTX/FMN-NPs was in the same pattern. In the meantime, FMN release from HA-DTX/FMN-NPs was relatively faster.

Cellular Uptake

The cellular uptake efficiency of dual ligand-modified HA/GE-DTX/FMN-NPs and HA/GE-NPs was around 60% (Figure 4), which was higher compared with GE-DTX/FMN-NPs (48.9%) and HA-DTX/FMN-NPs (38.3%) ($P < 0.05$). GE-DTX/FMN-NPs showed higher cancer cell uptake ability than HA-DTX/FMN-NPs.

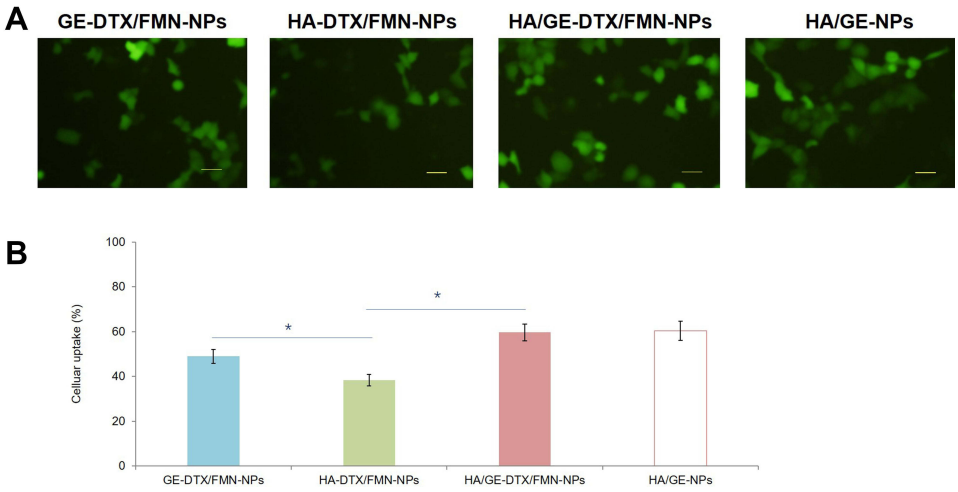

Figure 4 Cellular uptake efficiency of the coumarin 6-loaded NPs in PC3 cells: fluorescence images (**A**) and quantified by flow cytometer (**B**). Bars stand for 50 μm. Data are presented as means ± standard deviation (*n*=3). *$P < 0.05$.

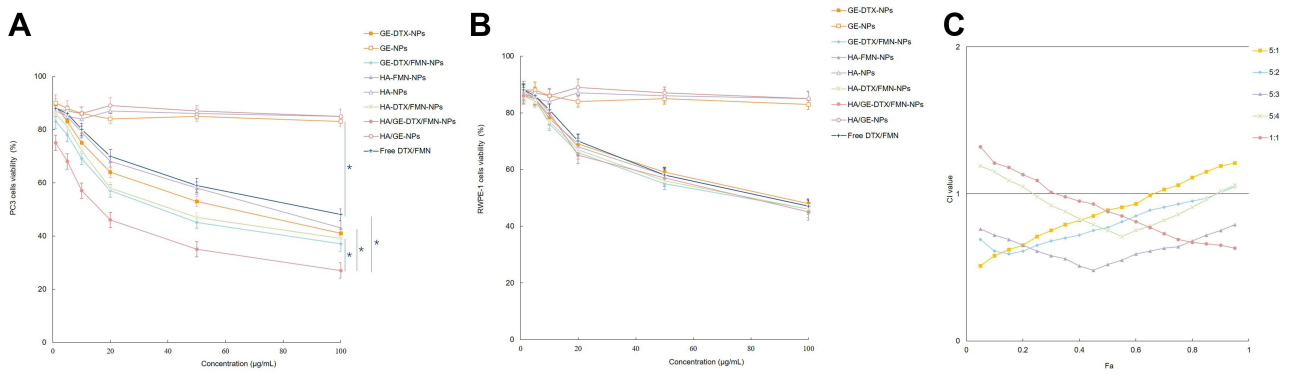

Figure 5 In vitro cytotoxicity of different formulations on PC3 cells (**A**) and RWPE-1 cells (**B**). CI values versus Fa at different DTX to FMN ratios (**C**). Data are presented as means ± standard deviation (n=3). *P < 0.05.

In vitro Cytotoxicity and Synergistic Effect

In vitro cytotoxicity of NPs was evaluated on PCa cells (PC3 cells) and normal cells (RWPE-1 cells), respectively. Figure 5 A shows that HA/GE-DTX/FMN-NPs inhibited PC3 cells more efficiently compared with single ligand-modified NPs (GE-DTX/FMN-NPs and HA-DTX/FMN-NPs, $P < 0.05$), single drug-loaded NPs (GE-DTX-NPs and HA-FMN-NPs, $P < 0.05$), and free DTX/FMN ($P < 0.05$). In contrast, NPs and free drugs showed no remarkable difference on normal RWPE-1 cells (Figure 5B). Figure 5C summarizes the CI values versus the fraction of the affected cells (Fa) at different DTX to FMN ratios. CI values below 1 were found at a molar ratio of 5:3 (DTX:FMN, w/w), indicating the synergy of the two drugs at this ratio.

In vivo Anti-Tumor Efficacy and Biodistribution

HA/GE-DTX/FMN-NPs showed significantly higher tumor inhibition efficiency compared with single ligand-modified GE-DTX/FMN-NPs and HA-DTX/FMN-NPs (Figure 6, $P < 0.05$). Double drug co-loaded GE-DTX/FMN-NPs and HA-DTX/FMN-NPs exhibited remarkably better antitumor ability than their single drug-loaded counterparts (GE-DTX-NPs and HA-FMN-NPs) and free DTX/FMN ($P < 0.05$). The tumor images are also presented in Figure 6. In vivo

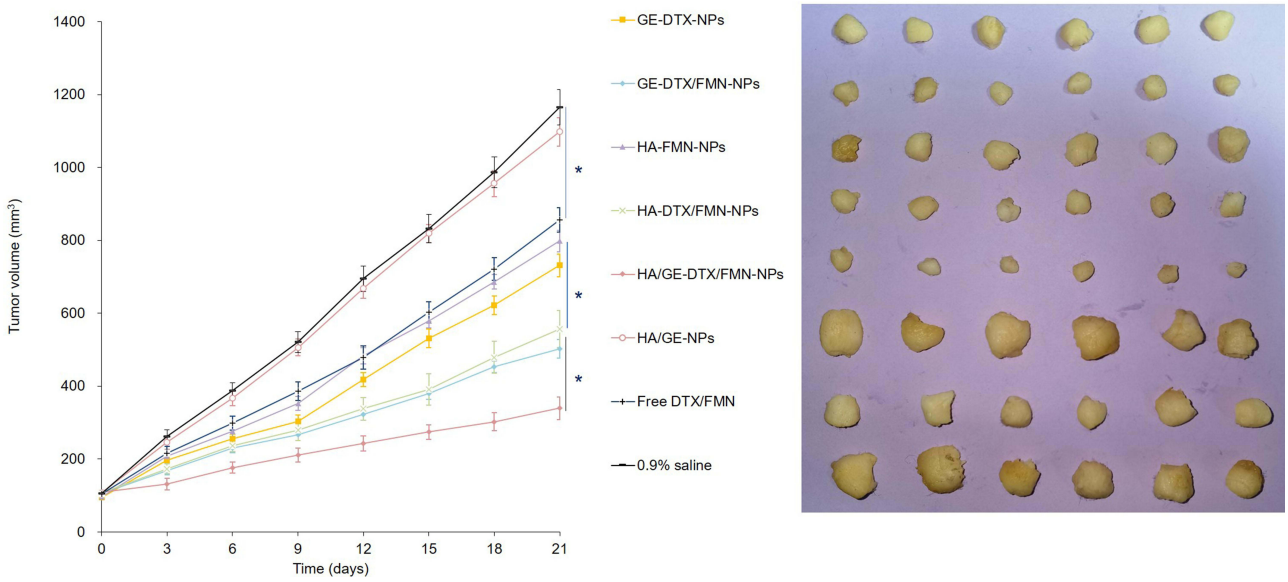

Figure 6 In vivo anti-tumor efficacy of different formulations in mice bearing human prostate cancer model: Tumor volumes and images. Data are presented as means ± standard deviation (n=8). *P < 0.05.

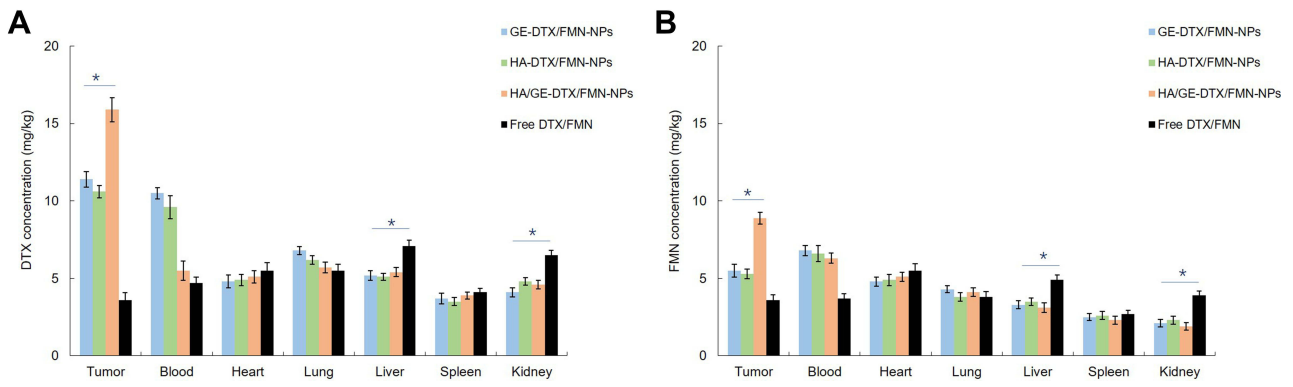

Figure 7 In vivo DTX (**A**) and FMN (**B**) tissue distribution. Data are presented as means ± standard deviation (n=8). *P < 0.05.

biodistribution results illustrated that HA/GE-DTX/FMN-NPs distributed more in tumor compared with GE-DTX/FMN-NPs and HA-DTX/FMN-NPs (Figure 7, $P < 0.05$). Double drug co-loaded NPs showed higher tumor drug distribution than free DTX/FMN ($P < 0.05$). Of note, free DTX/FMN distributed more drugs in liver and kidney compared with NPs groups ($P < 0.05$).

Discussion

The aim of this study was to construct GE11 and HA dual ligand co-modified, DTX and FMN co-loaded binary nanoparticles to facilitate PCa combination therapy. Firstly, anionic and bio-adhesive GE-NPs were prepared using Carbopol 940 (CP) as a surfactant. Zou et al had reported that CP could enhance the bio-adhesion effect of PLGA nanoparticles to treat lung cancer.[36] In this study, PLGA-PEG-GE11 was used to prepare GE-DTX-NPs with a size of 100.3 nm and a zeta potential of −21.7 mV, and the resulting GE-DTX-NPs were used as the supporting core of the binary NPs. Secondly, cationic HA-FMN-NPs were prepared using DDAB as a surfactant. DDAB is a double-tailed surfactant which was reported to exhibit lower cytotoxicity compared with single-tailed cationic lipids such as cetyltrimethylammonium bromide (CTAB).[37] HA-FMN-NPs showed a size of 43.1 nm and a zeta potential of +33.9 mV. Finally, binary HA/GE-DTX/FMN-NPs were prepared through the adhesive attraction and electrical charge interaction between HA-FMN-NPs and GE-DTX-NPs. The bio-adhesive cationic GE-DTX-NPs could be the inner core that adhere anionic HA-FMN-NPs onto its surface. TEM images showed that binary HA/GE-DTX/FMN-NPs exhibited some smaller particles coating on the inner core and achieved an enlarged size of 189.5 nm, which is larger than that of HA-FMN-NPs and GE-DTX-NPs.

It was reported that particle sizes smaller than 200 nm are conducive to drug accumulation at the tumor site by the enhanced permeation and retention (EPR) effect.[38]

Zeta potential can affect nanoparticle phagocytosis or pharmacokinetic characteristics.[39] Positive zeta potential cationic NPs, compared to negatively charged NPs, have greater affinity to cell membranes. The anionic lipid components in the internal cancer cell membrane make the cell surface negatively charged. Negative charges of the tumor vasculature's endothelial cell membranes might have potentiated the electrostatic activity between positively charged nanoparticles and the tumor. The NPs were stable during 3 months of storage and 72 h in the presence of serum, suggesting that this formulation will not aggregate or disassemble after intravenous administration for 3 days, and the storage conditions are suitable for the NPs.[38]

The drug release pattern from a delivery system could be affected by several factors such as physicochemical properties of entrapped drugs, nature of the core, strength of the interactions between the drugs, and the shell materials.[39] Drug release from GE-DTX/FMN-NPs was slower than that of HA-DTX/FMN-NPs, which may be explained by the polymeric PLGA NPs being able to hold the drugs for a longer time compared with lipid NPs. DTX release from HA/GE-DTX/FMN-NPs was slower than from GE-DTX/FMN-NPs, and this could be the evidence that the coating of HA-FMN-NPs on the surface of GE-DTX-NPs hindered the DTX release from the inner core.

The therapeutic effects of the drug-loaded NPs depend on the uptake by cancer cells.[40] Coumarin 6 is a fluorescent probe, which was reported to represent the drug in the nanoparticle formulation to analyze cellular uptake of the NPs.[41] Based on the qualitative and quantitative results of the cellular uptake, dual ligand-modified HA/GE-DTX/FMN-NPs showed significantly higher uptake efficiency compared with GE-DTX/FMN-NPs and HA-DTX/FMN-NPs, indicating that the HA and GE modification could cause the dual-targeting capacity of the NPs to PCa cells.

In vitro cytotoxicity of both drug-loaded NPs and free drugs was reported to reduce cell viability in a concentration-dependent manner by Zhang et al.[43] In this study, similar results were found that the cytotoxicity of samples increased along with the concentrations. The higher cytotoxicity of drug-loaded NPs was found to be better than free drug, indicating that NPs delivery systems can enhance the cytotoxicity on PC3 cells. In the contrast, NPs and free drugs showed no remarkable difference on normal RWPE-1 cells. This result is in line with the experiments carried out by Song et al, who found negligible difference of cytotoxicity between free drugs and drug-contained NPs when evaluated on normal cells.[42] Evaluation of drug–drug interaction is important in combination cancer chemotherapy,[43] and CI values were evaluated to determine the optimized drugs ratio for the preparation of NPs.[33] When the DTX:FMN ratio is 5:3 (w/w), the lowest CI curve was achieved, which is below 1. According to the results, DTX (50 mg) and FMN (30 mg) were used for the combined drug systems.

In tumor tissues, the formation of leaky vessels and pores (100 nm to 2 μm in diameter) and the poor lymphatic system offers great opportunity to treat cancer, which is known as the enhanced permeability and retention (EPR) effect.[44] Jin et al argued that the nano-sized carriers could facilitate the delivery of drugs to the tumor site. In vivo biodistribution results in this study are proof that NPs distributed more in tumor compared with free drugs. Free DTX/FMN distributed more drugs in liver and kidney compared with NPs groups, which could be the evidence of the less systemic toxicity of the NPs systems.[45] HA/GE-DTX/FMN-NPs showed significantly higher tumor inhibition efficiency compared with single ligand-modified GE-DTX/FMN-NPs and HA-DTX/FMN-NPs, which is in accordance with the results of Xu et al.[47] They concluded that the dual ligand modification led to a significant benefit relative to the use of one ligand alone. Double drug co-loaded GE-DTX/FMN-NPs and HA-DTX/FMN-NPs exhibited remarkable antitumor ability compared to single drug-loaded GE-DTX-NPs and HA-FMN-NPs, which is also concluded by Jiang et al.[46] They proved that if the drugs loaded in the NPs have a synergistic effect, the dosage of both drugs could be reduced, which could help with the reduction of unexpected side effects during the cancer therapy procedure and also bring about excellent anti-tumor efficiency.

Conclusion

Binary HA/GE-DTX/FMN-NPs were designed in this study. They were nano-sized particles with smaller particles coating on the inner core and achieved a size of 189.5 nm. HA/GE-DTX/FMN-NPs showed a cellular uptake efficiency of 59.6%, and a more efficient inhibition effect on PC3 cells compared with single ligand-modified NPs and free drugs. HA/GE-DTX/FMN-NPs showed significantly higher tumor inhibition efficiency than their single drug-loaded counterparts and free drugs. HA/GE-DTX/FMN-NPs have a synergistic anti-tumor effect and also could reduce unexpected side effects during the cancer therapy. It could be used as a promising anti-PCa system.

Acknowledgement

This work is supported by Cultivation Fund of the 2nd Hospital of Shandong University (2022YP77).

Disclosure

The authors report no conflicts of interest in this work.

References

1. Bray F, Ferlay J, Soerjomataram I, Siegel RL, Torre LA, Jemal A. Global cancer statistics 2018: GLOBOCAN estimates of incidence and mortality worldwide for 36 cancers in 185 countries. *CA Cancer J Clin*. 2018;68(6):394–424. doi:10.3322/caac.21492
2. Cassell A, Yunusa B, Jalloh M, et al. Management of advanced and metastatic prostate cancer: a need for a sub-saharan guideline. *J Oncol*. 2019;2019:1785428. doi:10.1155/2019/1785428

3. Horwich A, Parker C, Kataja V; ESMO Guidelines Working Group. Prostate cancer: ESMO clinical recommendations for diagnosis, treatment and follow-up. *Ann Oncol*. 2009;20(Suppl 4):76–78. doi:10.1093/annonc/mdp135
4. National Comprehensive Cancer Network: NCCN clinical prastice guidelines in oncology (NCCN Guidelines®): prostate cancer V.2.2021. National Comprehensive Cancer Network, Inc. Available from: https://www.nccn.org/guidelines/guidelines-detail?category=1&id=1459. Accessed July 29, 2022.
5. Oudard S. TROPIC: phase III trial of cabazitaxel for the treatment of metastatic castration-resistant prostate cancer. *Future Oncol*. 2011;7(4):497–506. doi:10.2217/fon.11.23
6. Petrylak DP, Tangen CM, Hussain MH, et al. Docetaxel and estramustine compared with mitoxantrone and prednisone for advanced refractory prostate cancer. *N Engl J Med*. 2004;351(15):1513–1520. doi:10.1056/NEJMoa041318
7. Berthold DR, Pond GR, Soban F, de Wit R, Eisenberger M, Tannock IF. Docetaxel plus prednisone or mitoxantrone plus prednisone for advanced prostate cancer: updated survival in the TAX 327 study. *J Clin Oncol*. 2008;26(2):242–245. doi:10.1200/JCO.2007.12.4008
8. Cho H-J, Yoon HY, Koo H, et al. Self-assembled nanoparticles based on hyaluronic acid-ceramide (HA-CE) and Pluronic® for tumor-targeted delivery of docetaxel. *Biomaterials*. 2011;32(29):7181–7190. doi:10.1016/j.biomaterials.2011.06.028
9. Tanaudommongkon I, Tanaudommongkon A, Prathipati P, Nguyen JT, Keller ET, Dong X. Curcumin nanoparticles and their cytotoxicity in docetaxel-resistant castration-resistant prostate cancer cells. *Biomedicines*. 2020;8(8):253. doi:10.3390/biomedicines8080253
10. Barani M, Sabir F, Rahdar A, Arshad R, Kyzas GZ. Nanotreatment and nanodiagnosis of prostate cancer: recent updates. *Nanomaterials*. 2020;10(9):1696. doi:10.3390/nano10091696
11. Yan J, Wang Y, Zhang X, Liu S, Tian C, Wang H. Targeted nanomedicine for prostate cancer therapy: docetaxel and curcumin co-encapsulated lipid-polymer hybrid nanoparticles for the enhanced anti-tumor activity in vitro and in vivo. *Drug Deliv*. 2016;23(5):1757–1762. doi:10.3109/10717544.2015.1069423
12. Zhang Y, Lei BH, Zou Q, Zhu QY, Lu ZJ, Wang Y. 张扬, 雷博涵, 邹青, 朱清毅, 卢子杰, 汪悦.中西医结合治疗去势抵抗性前列腺癌的疗效观察.中华男科学杂志. [Clinical efficacy of integrated traditional Chinese and Western medicine for castration-resistant prostate cancer]. *Zhonghua Nan Ke Xue*. 2017;23(10):922–927. Chinese.
13. Markowitsch SD, Juetter KM, Schupp P, et al. Shikonin reduces growth of docetaxel-resistant prostate cancer cells mainly through necroptosis. *Cancers*. 2021;13(4):882. doi:10.3390/cancers13040882
14. Fu W, Hong Z, You X, et al. Enhancement of anticancer activity of docetaxel by combination with Fuzheng Yiliu decoction in a mouse model of castration-resistant prostate cancer. *Biomed Pharmacother*. 2019;118:109374. doi:10.1016/j.biopha.2019.109374
15. Singh SP, Wahajuddin YDK, Rawat P, Maurya R, Jain GK. Quantitative determination of formononetin and its metabolite in rat plasma after intravenous bolus administration by HPLC coupled with tandem mass spectrometry. *J Chromatogr B Analyt Technol Biomed Life Sci*. 2010;878(3–4):391–397. doi:10.1016/j.jchromb.2009.12.010
16. Wang AL, Li Y, Zhao Q, Fan LQ. Formononetin inhibits colon carcinoma cell growth and invasion by microRNA-149-mediated EphB3 downregulation and inhibition of PI3K/AKT and STAT3 signaling pathways. *Mol Med Rep*. 2018;17(6):7721–7729. doi:10.3892/mmr.2018.8857
17. Jarred RA, Keikha M, Dowling C, et al. Induction of apoptosis in low to moderate-grade human prostate carcinoma by red clover-derived dietary isoflavones. *Cancer Epidemiol Biomarkers Prev*. 2002;11(12):1689–1696.
18. Ong SKL, Shanmugam MK, Fan L, et al. Focus on formononetin: anticancer potential and molecular targets. *Cancers*. 2019;11(5):611. doi:10.3390/cancers11050611
19. Ye Y, Hou R, Chen J, et al. Formononetin-induced apoptosis of human prostate cancer cells through ERK1/2 mitogen-activated protein kinase inactivation. *Horm Metab Res*. 2012;44(4):263–267. doi:10.1055/s-0032-1301922
20. Huang WJ, Bi LY, Li ZZ, Zhang X, Ye Y. Formononetin induces the mitochondrial apoptosis pathway in prostate cancer cells via downregulation of the IGF-1/IGF-1R signaling pathway. *Pharm Biol*. 2013. PMID: 24359236. doi:10.3109/13880209.2013.842600
21. Liu XJ, Li YQ, Chen QY, Xiao SJ, Zeng SE. Up-regulating of RASD1 and apoptosis of DU-145 human prostate cancer cells induced by formononetin in vitro. *Asian Pac J Cancer Prev*. 2014;15(6):2835–2839. doi:10.7314/APJCP.2014.15.6.2835
22. Li T, Zhao X, Mo Z, et al. Formononetin promotes cell cycle arrest via downregulation of Akt/Cyclin D1/CDK4 in human prostate cancer cells. *Cell Physiol Biochem*. 2014;34(4):1351–1358. doi:10.1159/000366342
23. Yan J, Wang Y, Jia Y, et al. Co-delivery of docetaxel and curcumin prodrug via dual-targeted nanoparticles with synergistic antitumor activity against prostate cancer. *Biomed Pharmacother*. 2017;88:374–383. doi:10.1016/j.biopha.2016.12.138
24. Souchek JJ, Wojtynek NE, Payne WM, et al. Hyaluronic acid formulation of near infrared fluorophores optimizes surgical imaging in a prostate tumor xenograft. *Acta Biomater*. 2018;75:323–333. doi:10.1016/j.actbio.2018.06.016
25. Qu Z, Ren Y, Shen H, Wang H, Shi L, Tong D. Combination therapy of metastatic castration-recurrent prostate cancer: hyaluronic acid decorated, cabazitaxel-prodrug and orlistat co-loaded nano-system. *Drug Des Devel Ther*. 2021;15:3605–3616. doi:10.2147/DDDT.S306684
26. Jin Y, Wang Y, Liu X, et al. Synergistic combination chemotherapy of lung cancer: cisplatin and doxorubicin conjugated prodrug loaded, glutathione and pH sensitive nanocarriers. *Drug Des Devel Ther*. 2020;14:5205–5215. doi:10.2147/DDDT.S260253
27. Chen G, Zhang Y, Deng H, Tang Z, Mao J, Wang L. Pursuing for the better lung cancer therapy effect: comparison of two different kinds of hyaluronic acid and nitroimidazole co-decorated nanomedicines. *Biomed Pharmacother*. 2020;125:109988. doi:10.1016/j.biopha.2020.109988
28. Wang L, Liu Z, Liu D, Liu C, Juan Z, Zhang N. Docetaxel-loaded-lipid-based-nanosuspensions (DTX-LNS): preparation, pharmacokinetics, tissue distribution and antitumor activity. *Int J Pharm*. 2011;413(1–2):194–201. doi:10.1016/j.ijpharm.2011.04.023
29. Wang C, Su L, Wu C, Wu J, Zhu C, Yuan G. RGD peptide targeted lipid-coated nanoparticles for combinatorial delivery of sorafenib and quercetin against hepatocellular carcinoma. *Drug Dev Ind Pharm*. 2016;42(12):1938–1944. doi:10.1080/03639045.2016.1185435
30. Dong Z, Guo J, Xing X, Zhang X, Du Y, Lu Q. RGD modified and PEGylated lipid nanoparticles loaded with puerarin: formulation, characterization and protective effects on acute myocardial ischemia model. *Biomed Pharmacother*. 2017;89:297–304.
31. Guo J, Xing X, Lv N, et al. Therapy for myocardial infarction: in vitro and in vivo evaluation of puerarin-prodrug and tanshinone co-loaded lipid nanoparticulate system. *Biomed Pharmacother*. 2019;120:109480. doi:10.1016/j.biopha.2019.109480
32. Liu C, Liu F, Feng L, Li M, Zhang J, Zhang N. The targeted co-delivery of DNA and doxorubicin to tumor cells via multifunctional PEI-PEG based nanoparticles. *Biomaterials*. 2013;34(10):2547–2564. doi:10.1016/j.biomaterials.2012.12.038
33. Liang Z, Li J, Zhu B. Lung cancer combination treatment: evaluation of the synergistic effect of cisplatin prodrug, vinorelbine and retinoic acid when co-encapsulated in a multi-layered nano-platform. *Drug Des Devel Ther*. 2020;14:4519–4531. doi:10.2147/DDDT.S251749

34. Chou TC, Talalay P. Generalized equations for the analysis of inhibitions of Michaelis-Menten and higher-order kinetic systems with two or more mutually exclusive and nonexclusive inhibitors. *Eur J Biochem*. 1981;115(1):207–216. doi:10.1111/j.1432-1033.1981.tb06218.x
35. Fan X, Wang T, Ji Z, Li Q, Shen H, Wang J. Synergistic combination therapy of lung cancer using lipid-layered cisplatin and oridonin co-encapsulated nanoparticles. *Biomed Pharmacother*. 2021;141:111830. doi:10.1016/j.biopha.2021.111830
36. Zou W, Liu C, Chen Z, Zhang N. Studies on bioadhesive PLGA nanoparticles: a promising gene delivery system for efficient gene therapy to lung cancer. *Int J Pharm*. 2009;370(1–2):187–195. doi:10.1016/j.ijpharm.2008.11.016
37. Yu W, Liu C, Ye J, Zou W, Zhang N, Xu W. Novel cationic SLN containing a synthesized single-tailed lipid as a modifier for gene delivery. *Nanotechnology*. 2009;20(21):215102. doi:10.1088/0957-4484/20/21/215102
38. Hong Y, Che S, Hui B, Wang X, Zhang X, Ma H. Combination therapy of lung cancer using layer-by-layer cisplatin prodrug and curcumin co-encapsulated nanomedicine. *Drug Des Devel Ther*. 2020;14:2263–2274. doi:10.2147/DDDT.S241291
39. Rahman M, Almalki WH, Afzal O, et al. Cationic solid lipid nanoparticles of resveratrol for hepatocellular carcinoma treatment: systematic optimization, in vitro characterization and preclinical investigation. *Int J Nanomedicine*. 2020;15:9283–9299. doi:10.2147/IJN.S277545
40. Tan S, Wang G. Redox-responsive and pH-sensitive nanoparticles enhanced stability and anticancer ability of erlotinib to treat lung cancer in vivo. *Drug Des Devel Ther*. 2017;11:3519–3529. doi:10.2147/DDDT.S151422
41. Chandratre SS, Dash AK. Multifunctional nanoparticles for prostate cancer therapy. *AAPS PharmSciTech*. 2015;16(1):98–107. doi:10.1208/s12249-014-0202-z
42. Hong Y, Che S, Hui B, et al. Lung cancer therapy using doxorubicin and curcumin combination: targeted prodrug based, pH sensitive nanomedicine. *Biomed Pharmacother*. 2019;112:108614. doi:10.1016/j.biopha.2019.108614
43. Zhang R, Ru Y, Gao Y, Li J, Mao S. Layer-by-layer nanoparticles co-loading gemcitabine and platinum (IV) prodrugs for synergistic combination therapy of lung cancer. *Drug Des Devel Ther*. 2017;11:2631–2642. doi:10.2147/DDDT.S143047
44. Song Z, Shi Y, Han Q, Dai G. Endothelial growth factor receptor-targeted and reactive oxygen species-responsive lung cancer therapy by docetaxel and resveratrol encapsulated lipid-polymer hybrid nanoparticles. *Biomed Pharmacother*. 2018;105:18–26. doi:10.1016/j.biopha.2018.05.095
45. Wang J. Combination treatment of cervical cancer using folate-decorated, pH-sensitive, carboplatin and paclitaxel co-loaded lipid-polymer hybrid nanoparticles. *Drug Des Devel Ther*. 2020;14:823–832. doi:10.2147/DDDT.S235098
46. Cui T, Zhang S, Sun H. Co-delivery of doxorubicin and pH-sensitive curcumin prodrug by transferrin-targeted nanoparticles for breast cancer treatment. *Oncol Rep*. 2017;37(2):1253–1260.
47. Xu G, Chen Y, Shan R, Wu X, Chen L. Transferrin and tocopheryl-polyethylene glycol-succinate dual ligands decorated, cisplatin loaded nano-sized system for the treatment of lung cancer. *Biomed Pharmacother*. 2018;99:354–362. doi:10.1016/j.biopha.2018.01.062